Journal of Applied Polymer Science

Acetamide-Modified Hyper-Cross-Linked Resin: Synthesis, Characterization, and Adsorption Performance to Phenol from Aqueous Solution

Xiaomei Wang,[1,2] Prafulla D. Patil,[1] Chunlian He,[3] Jianhan Huang,[1] You-Nian Liu[1]

[1]College of Chemistry and Chemical Engineering, Central South University, Changsha, Hunan 410083, China
[2]Department of Bioengineering and Environmental Science, Changsha University, Changsha, Hunan 410003, China
[3]Medicine College, Hunan Normal University, Changsha, Hunan 410081, China
Correspondence to: C. He (E-mail: chunlianhe69@163.com) and Y.-N. Liu (E-mail: jianhanhuang@csu.edu.cn or liuyounian@csu.edu.cn)

ABSTRACT: Acetamide-modified hyper-cross-linked resin, HCP-HMTA-AA, was prepared and its adsorption performance was evaluated using phenol as the adsorbate. The prepared HCP–HMTA–AA owned predominant micro/mesopores and medium polarity, making it possess a superior adsorption to phenol as compared with polystyrene (PS), chloromethylated polystyrene (CMPS), hyper-cross-linked polymer (HCP) and amino-modified hyper-cross-linked resin (HCP–HMTA). The adsorption enthalpy was −99.56 kJ/mol at zero fractional loading, multiple hydrogen bonding contributed to such a great adsorption enthalpy and an approximately planar hexahydric ring was formed between acetamide of HCP–HMTA–AA and phenol. The dynamic capacity of phenol on HCP–HMTA–AA was 291.3 mg/g at a feed concentration of 946.2 mg/L and a flow rate of 48 mL/h and the resin column was almost regenerated by a mixed solvent including 50% of ethanol (v/v) and 0.01 mol/L of sodium hydroxide (w/v). HCP–HMTA–AA was repeatedly used for five times and the equilibrium adsorption capacity for the five time reached 94.2% of the equilibrium adsorption capacity for the first time. © 2014 Wiley Periodicals, Inc. J. Appl. Polym. Sci. **2015**, *132*, 41597.

KEYWORDS: adsorption; copolymers; polystyrene; porous materials

Received 26 July 2014; accepted 6 October 2014
DOI: 10.1002/app.41597

INTRODUCTION

Phenol and its derivatives are widely used in petrochemical, oil refining, plastics, leather, pharmaceutical and pesticides industries,[1,2] and they are inevitably existent in the effluents from these industries. Sometimes, the concentration of phenol in the wastewater is very high, For instance, the concentration of phenol in the oil refinery processes and coking plants exceeds 1000 mg/dm.[3] Phenol and its derivatives are the priority pollutants in environment because they are associated with intensely acute and chronic toxic effects on human health.[3] For example, phenol is a potential carcinogen, and it can result in headache, vomiting, fainting and other mental disorders, which can cause profound health and environmental problems. As a result, effective removal of phenol and its derivatives from wastewater has increasingly become an essential environmental concern, and hence attracted many interests in recent years.[4,5]

Many methods including solvent extraction, catalytic degradation, biodegradation, chemical oxidation, membrane separation, and adsorption are employed for removal of phenol from wastewater, and among which adsorption is the most promising physical method for removal of phenol and its derivatives from aqueous solution. Activated carbon is proven an excellent organic adsorbent.[6,7] Activated carbon has a very high Brunauer-Emmet-Teller (BET) surface area, pore volume and predominantly abundant micropores, which result in a very large equilibrium adsorption capacity to phenol and its derivatives. However, the used activated carbon is difficult to regenerate, and its mechanical strength is poor after repeated use. Hence, it is important to look for an alternative adsorbent to take the place of activated carbon for adsorptive removal of phenol and its derivatives from aqueous solution.

In 1969, Davankov et al proposed a fundamentally novel approach for preparation of a kind of novel cross-linked polystyrene (PS),[8,9] this kind of cross-linked PS is frequently termed as hyper-cross-linked polymer (HCP). HCP is found very effective for removing phenol and its derivatives from aqueous solution.[10,11] In addition, HCP has strong mechanical strength, and it can be easily regenerated for repeated use and reused for more than 50 cycles. Hence, it is being considered as a potential replacement of activated carbon for adsorptive removal of phenol and its derivatives from wastewater.

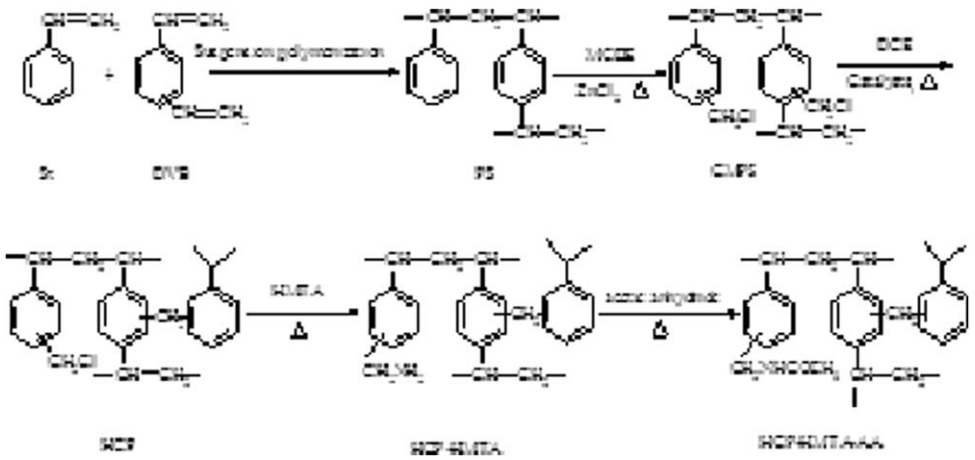

Scheme 1. Synthetic procedure for the acetamide-modified hyper-cross-linked resin, HCP–HMTA–AA.

HCP is generally synthesized from linear PS or low cross-linked PS with bi-functional cross-linking reagents in the presence of Friedel-Crafts catalysts.[9] Bis-chloromethyl derivatives such as *p*-xylylene dichloride (XDC), 1,4-bis-(chloromethyl)-diphenyl (CMDP) and 1,3,5-tris-(chloromethyl)mesitylene (CMM) are found the preferable bi-functional cross-linking reagents,[12–15] and anhydrous aluminum chloride, iron (III) chloride, zinc chloride and stannic (IV) chloride are shown the excellent Friedel-Crafts catalysts. Monochlorodimethyl ether (MCDE) can react with low cross-linked PS quantitatively through a typical chloromethylation reaction, and the introduced chloromethyl groups on PS can further react with another phenyl ring by the Friedel-Crafts reaction under the help of Friedel-Crafts catalysts at a higher temperature, resulting in post-cross-linking of the PS and formation of HCP.[14,16,17] The obtained HCP consists of an intensive bridging of strongly solvated PS chains with conformationally rigid cross-linking, and the pore diameter distribution transfers from predominant mesopores to mesopores-micropores bimodal distribution,[18,19] and hence results in a great increase of the BET surface area and pore volume.[20–22] Because of these significant changes, HCP possesses large equilibrium adsorption capacity to phenol and its derivatives from aqueous solution.

To improve the polarity of HCP and increase the equilibrium adsorption capacity of HCP to polar organic compounds, it is often chemically modified by introduction of polar units into the copolymers, using polar compounds as the cross-linking reagent and addition of polar compounds in the Friedel-Crafts reaction.[23–25] Acetamide groups are efficient functional groups for improving the equilibrium adsorption capacity of polymeric adsorbent due to formation of possible hydrogen bond between the acetamide groups and the adsorbate.[26–29] If acetamide groups can be modified on the surface of HCP, in addition to the excellent pore structure of HCP, the polarity matching between the chemically modified HCP and the adsorbate will also have an advantageous effect on the adsorption. Hence, a novel HCP functionalized by acetamide groups was synthesized in the present study, and the adsorption behaviors of the obtained HCP was evaluated using phenol as the adsorbate, the adsorption equilibrium and breakthrough dynamics were measured and analyzed in detail.

MATERIALS AND METHOD

Materials

Styrene (St) and divinylbenzene (DVB, purity: 80 wt %) was purchased from Gray West Chengdu Chemical Technology (Sichuan Province, China), they were washed by 5% of sodium hydroxide (w/v) and water until neutral pH, and then dried by anhydrous magnesium sulfate before use. Toluene, liquid paraffin, petroleum ether, MCDE (high toxicity to the health, it should be used very carefully in the experiment), anhydrous zinc chloride ($ZnCl_2$), 1,2-dichloroethane (DCE), N,N-dimethylformamide (DMF), hexamethylenetetramine (HMTA), potassium iodide (KI), and acetic anhydride were used in this study, these chemicals are of analytical grade and used without further purification. Phenol applied as the adsorbate in this study was an analytical reagent and used after distillation.

Synthesis of the Acetamide-Modified Hyper-Cross-Linked Resin

The preparation procedure for the acetamide-modified hyper-cross-linked resin, HCP–HMTA–AA, was described in Scheme 1. Macroporous cross-linked PS was prepared by a conventional suspension polymerization according to the method in Ref. 30. St and DVB were used as the monomers in the polymerization and the cross-linking degree of the obtained PS was 6% (w/w). A mixture of toluene and liquid paraffin (w/w = 1 : 1) was used as porogens, and the ratio of the porogens to the monomers were 1.5 : 1 (w/w). The resultant PS beads were rinsed by hot water, cold water, extracted by petroleum ether for 20 h, and dried at 323 K for 8 h. Macroporous cross-linked PS was chloromethylated by MCDE following the method accounted in Ref. 31, anhydrous $ZnCl_2$ was employed as the catalysts and after this reaction macroporous cross-linked chloromethylated polystyrene (CMPS) was prepared. The Friedel-Crafts reaction of CMPS was performed following an established procedure[32] and HCP was produced after this reaction.

For amination of HCP,[33] 11.2 g of HMTA and 13.28 g of KI was dissolved in 200 mL of DMF to constitute a mixed

solution, which was applied to swell 20 g of HCP. The reaction solution was then heated to 373 K and kept at this temperature for 10 h. It was poured into deionized water, and the solids were filtered and successively eluted by 6 mol/L of hydrochloric acid (w/v), deionized water, 10% of sodium hydroxide (w/v) and deionized water until neutral pH. They were extracted by anhydrous ethanol for 10 h and dried at 323 K for 8 h, hence the resultant amino-modified hyper-cross-linked resin, HCP–HMTA, was synthesized. For the acetylation reaction,[26,29] HCP–HMTA was swollen by 80 mL of benzene and 25 mL of acetic anhydride at room temperature for 12 h, and the reaction mixture was refluxed for 10 h and hence the acetamide-modified hyper-cross-linked resin, HCP–HMTA–AA, was prepared.

Characterization of the Resins

The chorine content of the resin was measured by Volhard method.[31] The chorine element of the resins was decomposed to chloride ion by sodium hydroxide and potassium nitrate at a very high temperature, superfluous silver nitrate was applied to precipitate all of the chloride ion as a form of silver chloride, and then standard potassium thiocyanate solution was used to titrate the residual silver ion and ferric ammonium vanadium as employed as the indicator. The weak basic exchange capacity of the resin was determined by acid-base titration in ref. 30. Superfluous 0.1 mol/L of standard hydrochloric acid was used to make the $-NH_2$ group on the resins to $-NH_3^+$, and 0.1 mol/L of standard sodium hydroxide was used to titrate the residual hydrochloric acid and phenolphthalein was as employed as the indicator. The Fourier transformed infrared spectroscopy (FT-IR) of the resin was detected by KBr disks on a Nicolet 510P Fourier transformed infrared instrument. The BET surface area, t-plot micropore specific surface area, pore volume, t-plot micropore volume and pore diameter distribution of the resin were determined from N_2 adsorption–desorption isotherms at 77 K using a Micromeritics Tristar 3000 surface area and porosity analyzer. The total surface area and pore volume were calculated according to the BET model while the t-plot micropore surface area and t-plot micropore volume were calculated by the Barrett, Joyner and Halenda (BJH) method, and the pore diameter distribution was determined by applying BJH method to the N_2 desorption data. For calculation of the hydrogen bonding between HCP–HMTA–AA and phenol, Gaussian 03 program package was applied to predict the optimized molecular geometries of HCP–HMTA–AA, phenol, and the admixture of HCP–HMTA–AA with phenol.[26] Becke three parameter Lee-Yang-Parr (B3LYP) method with 6-311G basis set was performed for the calculation. N-methylacetamide was employed as the molecular analogue for HCP–HMTA–AA. The hydrogen bonding bond length, bond angle, dihedral angle of the plane of the molecular analogue with phenol, and bond energy were determined from the optimized structures of the admixture.

Equilibrium Adsorption

About 0.1 g of the resin was accurately weighed and mixed with a series of 50 mL of phenol solutions. The initial concentration of phenol solution was pre-set to be 201.4, 402.8, 604.2, 805.6, and 1007 mg/L, respectively. The original phenol solution is used without pH adjustment. The series of mixed solutions were shaken at a desired temperature (288, 293, 298, and 303 K, respectively) until adsorption equilibrium was reached after 4 h (the kinetic adsorption of the resin was performed, and 4 h were enough for the adsorption reaching equilibrium). The equilibrium concentration of phenol was determined and the accurate equilibrium adsorption capacity of phenol on the resin was calculated based on the differences of the concentration of phenol before and after the adsorption experiment.

Dynamic Adsorption and Desorption

3.34 g of the resin was accurately weighed and immersed in deionized water for 24 h. These wetted resins were then packed in a glass column ($\varphi = 16$ mm) densely to assembly a resin column (the volume of the wetted resin was 10 mL). A phenol solution at a feed concentration of 946.2 mg/L passed through the resin column at a flow rate of 48 mL/h and the concentration of phenol from the effluent, C (mg/L), was continuously recorded until it reached the feed concentration. After the breakthrough run, the resin column was rinsed by 10 mL of deionized water, and a mixed solvent including 50% of ethanol (v/v) and 0.01 mol/L of sodium hydroxide (w/v) were applied for regeneration of the resin. 100 mL of the mixed solvent passed through the resin column at a flow rate of 30 mL/h and the concentration of phenol was determined until it was zero.

RESULTS AND DISCUSSION

Characters of the Resins

The synthesized PS had the characteristic vibrational bands at 1600, 1500, and 1450 cm^{-1} (Figure 1), respectively, and which could be assigned to the C=C stretching of the phenyl groups. After the chloromethylation reaction, the chlorine content of CMPS was measured to be 17% (Table I), and a strong vibration, related to the C—Cl stretching of the chloromethyl groups, appeared at 1263 cm^{-1} in the FT-IR.[34] After the Friedel-Crafts reaction, the chlorine content of the resin sharply decreased to 3.9%, and the vibration of the C—Cl stretching was greatly weakened, demonstrating that most of the chlorine atoms of CMPS were consumed and the Friedel-Crafts reaction happened successfully. After amination reaction of HCP with HMTA, the chlorine content of the resin further decreased to 1.4%, whereas 0.70 mmol/g of weak basic exchange capacity (equals to 2.5% of chlorine content) was measured for the obtained HCP–HMTA, and the N—H deformation at 1500 cm^{-1} and N—H stretching in the range of 3926–3245 cm^{-1} appeared in the FT-IR.[35] These results indicated that a further nucleophilic substitution had taken place between the benzyl chloride of HCP and HMTA, and the $-NH_2$ groups were modified on the surface of HCP as the functional groups. After the acetylation reaction of HCP–HMTA with acetic anhydride, the weak basic exchange capacity of the resin decreased to 0.19 mmol/g, while a strong C=O stretching of acetamide at 1662 cm^{-1} emerged in the FT-IR,[26,29] implying that the $-NH_2$ groups were acetylated to $-NHCOCH_3$ by acetic anhydride. In conclusion, the acetamide-modified hyper-cross-linked resin, HCP–HMTA–AA, was prepared successfully in the present study, and its surface had 0.52 mmol/g of $-NHCOCH_3$ groups and 0.19 mmol/g of $-NH_2$ groups.

We tried to measure the N_2 adsorption–desorption isotherm of PS to obtain its pore structural parameters such as the BET

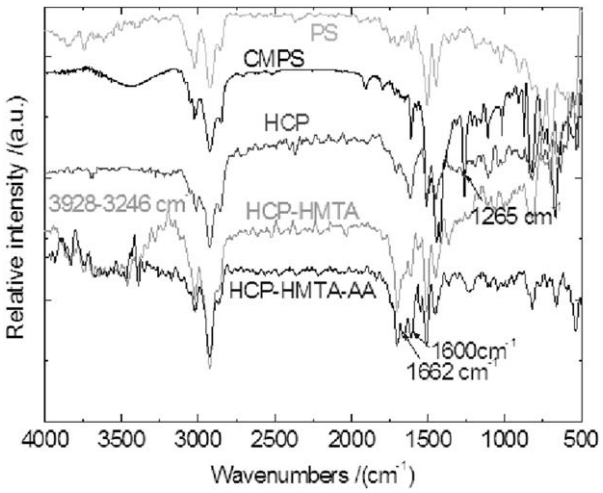

Figure 1. FT-IR spectra of PS, CMPS, HCP, HCP–HMTA, and HCP–HMTA–AA.

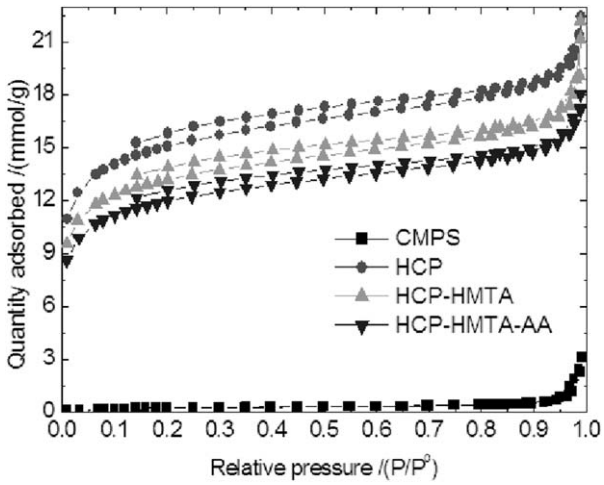

Figure 2. N_2 adsorption–desorption isotherms of CMPS, HCP, HCP–HMTA, and HCP–HMTA–AA.

surface area, pore volume and pore diameter distribution, but we failed. The BET surface area of CMPS was determined to be 18 m^2/g. The macro/mesopores in the range of 20–100 nm dominated the pores and a few super-micropores presented for CMPS. After the Friedel-Crafts reaction, the BET surface area and pore volume of HCP rapidly increased to 1052 m^2/g and 0.68 cm^3/g, respectively, and the N_2 adsorption capacity on HCP was much larger than CMPS at the same relative pressure (P/P^0) (Figure 2), suggesting that abundant methylene cross-linking bridges were formed in the Friedel-Crafts reaction.[12,14,20] This big change induced predominant micro/mesopores for HCP,[12,15] and 556 m^2/g of t-plot micropore surface area and 0.31 cm^3/g of t-plot micropore volume were measured. Additionally, the pore diameter distribution of HCP was divided by two regions, one is the micro/mesoporous region, which is dominant for HCP, and the other is the macroporous region (Figure 3).[19,21] The average pore diameter of the resin decreased from 25 nm to 2.7 nm. After the amination and acetylation of HCP, the BET surface area and pore volume were slightly decreased, which might be from the increased polarity due to the polar —NH_2 and —$NHCOCH_3$ groups on the surface.[32,36]

Table I. The Characteristic Parameters of CMPS, HCP, HCP-HMTA, and HCP-HMTA-AA

	CMPS	HCP	HCP-HMTA	HCP-HMTA-AA
BET surface area (m^2/g)	18	1052	925	859
Langmuir surface area (m^2/g)	28	1561	1411	1327
t-plot surface area (m^2/g)	-	556	526	539
Pore volume (cm^3/g)	0	0.68	0.59	0.55
t-plot pore volume (cm^3/g)	-	0.31	0.30	0.30
Average pore width (nm)	25	2.7	2.7	2.7
Chlorine content (%)	17	3.9	1.4	-
Weak basic exchange capacity (mmol/g)	-	-	0.70	0.19

Comparison of Phenol Adsorption on PS, CMPS, HCP, HCP–HMTA, and HCP–HMTA–AA

Figure 4 compares the equilibrium adsorption isotherms of phenol on PS, CMPS, HCP, HCP–HMTA, and HCP–HMTA–AA with the temperature at 288 K. The equilibrium adsorption capacity of phenol on HCP–HMTA–AA is proven the largest among the five resins. The BET surface area and pore volume of PS and CMPS were much lower than those of the three hyper-cross-linked resins, resulting in the much smaller equilibrium adsorption capacity. The BET surface area and pore volume of HCP–HMTA and HCP–HMTA–AA were a little lower than those of HCP, while the polar —NH_2 and —$NHCOCH_3$ groups on the resin could interact with phenol by static interaction and hydrogen bonding, and these polarity matching interaction enhanced the adsorption.[32,36] This result suggests that chemical modification of HCP by —NH_2 and —$NHCOCH_3$ groups on the surface of the resin is necessary.

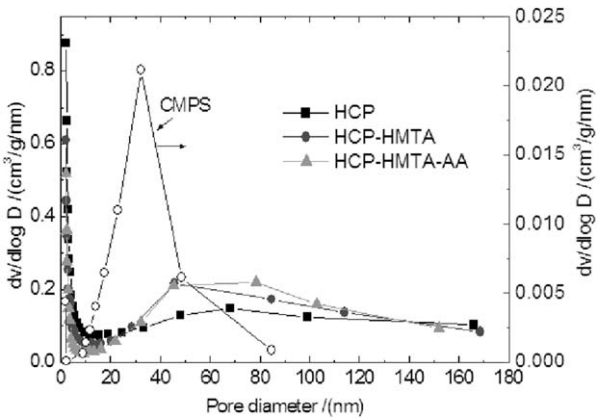

Figure 3. Pore diameter distribution of CMPS, HCP, HCP–HMTA, and HCP–HMTA–AA.

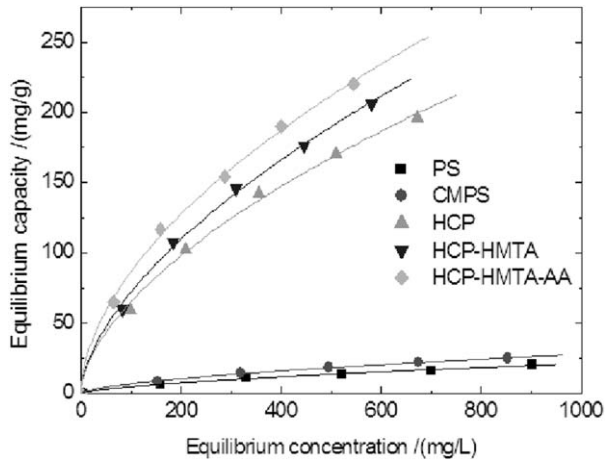

Figure 4. Comparison of equilibrium adsorption capacity of phenol on PS, CMPS, HCP, HCP–HMTA, and HCP–HMTA–AA (Resin weight: 0.1 g; volume of the solution: 50 mL; the initial concentration of phenol solution: 201.4, 402.8, 604.2, 805.6, and 1007 mg/L, respectively; $T = 288$ K).

At an equilibrium concentration of 100 mg/L, the equilibrium adsorption capacity of phenol on PS, CMPS, HCP, HCP–HMTA, and HCP–HMTA–AA is predicted to be 4.7, 6.8, 65, 73, and 87 mg/g, respectively. As compared the equilibrium adsorption capacity of phenol on HCP–HMTA–AA with some other acetamide-modified resins (Table II),[37,38] such as macroporous cross-linked N-methylacetamide-modified resin PMVBA,[26,27] macroporous cross-linked acetamide-modified resin PVBA[29] and N-methylacetamide-modified hyper-cross-linked resin HJ-Z01,[28] it is obvious that PMVBA, PVBA and HJ-Z01 are relatively inferior to HCP–HMTA–AA. PMVBA and PVBA are macroporous resins and had very small BET surface area and pore volume, and the phenol adsorption on these two resins is just driven by the polarity matching between the acetamide groups and phenol,[26,27,29] inducing a much low adsorption. HJ-Z01 is a N-methyacteamide-modified hyper-cross-linked resin and it gives the best phenol adsorption capacity among the polymeric adsorbents.[4,28] However, the equilibrium adsorption capacity of phenol on HJ-Z01 is shown a little smaller than HCP–HMTA–AA at the same equilibrium concentration and temperature. The BET surface area and pore volume of HJ-Z01 (839 m^2/g and 0.53 cm^3/g, respectively) are close to those of HCP–HMTA–AA (859 m^2/g and 0.55 cm^3/g, respectively), the t-plot micropore surface area and t-plot micropore volume of these two resins are roughly equal. Meanwhile, the loading amount of the functional groups on HJ-Z01 (0.64 mmol/g of $-N(CH_3)COCH_3$ groups and 0.18 mmol/g $-NHCH_3$ groups, respectively) is similar to HCP–HMTA–AA (0.52 mmol/g of $-NHCOCH_3$ groups and 0.19 mmol/g $-NH_2$ groups, respectively). The only difference of these two resins is that the acetamide groups. The acetamide groups on HJ-Z01 are $-N(CH_3)COCH_3$ groups, whereas those on HCP–HMTA–AA are $-NHCOCH_3$ groups and a hydrogen atom presents on the amino of acetamide groups for HCP–HMTA–AA. The further comparison of the equilibrium adsorption capacity of phenol on macroporous PMVBA and PVBA can also get the result that PVBA possesses a little larger equilibrium adsorption capacity of phenol than PMVBA, and the only difference between PMVBA and PVBA is that The acetamide groups on PMVBA are $-N(CH_3)COCH_3$ groups, whereas those on PVBA are $-NHCOCH_3$ groups. Hence, we deduce that this slight difference induces the quite different equilibrium adsorption capacity, and HCP–HMTA–AA possesses a larger equilibrium adsorption capacity.

Table II. Comparison of the Equilibrium Adsorption Capacity of the Polymeric Adsorbent at 100 mg/L of Equilibrium Concentration for the Adsorption of Phenol from Aqueous Solutions

Adsorbent	Equilibrium adsorption capacity of phenol	References
Polystyrene (PS)	4.7	This study
Chloromethylated polystyrene (CMPS)	6.8	This study
Hyper-cross-linked polymer (HCP)	65	This study
Aminated HCP (HCP-HMTA)	73	This study
Acetamidated HCP (HCP-HMTA-AA)	87	This study
N-methylacetamidated macroporous polystyrene (PMVBA)	34	26, 27
Acetamidated macroporous polystyrene (PVBA)	41	29
N-methylacetamidated HCP (HJ-Z01)	79	4, 28
Nitric acid modified activated carbons (WTAC)	28	37
Aminated activated carbons (ACN650)	110	38

Langmuir and Freundlich models are the two typical models for description of the adsorption.[39,40] The Langmuir model is the best-known model for description of the equilibrium adsorption. It assumes that the adsorption occurs on a structurally homogeneous adsorbent, and all the adsorption sites are energetically identical.[39] The Langmuir model can be expressed as:

$$q_e = \frac{K_L C_e q_m}{1 + K_L C_e} \quad (1)$$

where q_m is the maximum capacity (mg/g) of the adsorbate on the adsorbent and K_L is the Langmuir constant related to the adsorption affinity (L/g). It can be linearized as:

$$C_e/q_e = C_e/q_m + 1/(q_m \cdot K_L) \quad (2)$$

The Freundlich model is the earliest known model that describes the surface heterogeneity of the adsorbent.[40] It not only considers multilayer adsorption process but also considers multilayer adsorption process, and it can be arranged as:

Table III. The Fitted Parameters of the Isotherm Data for Phenol Adsorption on PS, CMPS, HCP, HCP-HMTA, and HCP-HMTA-AA According to the Linear Langmuir and Freundlich Models ($T = 288$ K)

	Langmuir model			Freundlich model		
	K_L (L/g)	q_m (mg/g)	R^2	K_F ([(mg/g)(L/mg)$^{1/n}$])	n	R^2
PS	1.229	36.74	0.9180	0.2324	1.529	0.9862
CMPS	1.459	44.64	0.9988	0.3285	1.547	0.9973
HCP	2.252	322.5	0.9982	3.094	1.595	0.9977
HCP-HMTA	2.511	340.1	0.9924	3.594	1.613	0.9968
HCP-HMTA-AA	3.653	373.1	0.9910	6.546	1.751	0.9970

$$q_e = K_F C_e^{1/n} \quad (3)$$

where K_F ([(mg/g)(L/mg)$^{1/n}$]) and n are the characteristic Freundlich constants. The linear Freundlich model can be displayed as:

$$\log q_e = (1/n)\log C_e + \log K_F \quad (4)$$

The linear Langmuir and Freundlich models were used to fit the isotherm data and the corresponding parameters q_m, K_L, K_F, and n, as well as the correlation coefficients (R^2) are summarized in Table III. It is obvious that both of the Langmuir and Freundlich models are suitable for fitting the equilibrium data and the Freundlich model is better for characterization of the adsorption due to the higher correlation coefficient ($R^2 > 0.98$). The corresponding K_F and n for the phenol adsorption on HCP–HMTA–AA is the greatest among the five resins,[40] implying that the adsorption on HCP–HMTA–AA is a more favorable process and the adsorption affinity of HCP–HMTA–AA to phenol is the strongest.

Equilibrium Adsorption

Figure 5 plots the equilibrium adsorption isotherms of phenol on HCP–HMTA–AA with the temperature at 288, 293, 298, and 303 K, respectively. It is clear that the equilibrium adsorption capacity decreases with increment of the temperature, implying that the adsorption is an exothermic process.[30] Table IV summarizes the corresponding parameters by fitting the equilibrium date by the Langmuir and Freundlich models. It is found that the isotherm data can be well fitted by both of the Langmuir and Freundlich models ($R^2 > 0.98$) and the Freundlich model is more suitable for fitting the equilibrium data ($R^2 > 0.99$). At the temperature of 288, 293, 298, and 303 K, the K_F are predicted to be 6.546, 6.111, 3.932, and 2.368 (mg/g)·(L/mg)$^{1/n}$, and the n are scaled to be 1.751, 1.748, 1.596, and 1.442, respectively, indicating that the adsorption at a higher temperature is less favorable.[40]

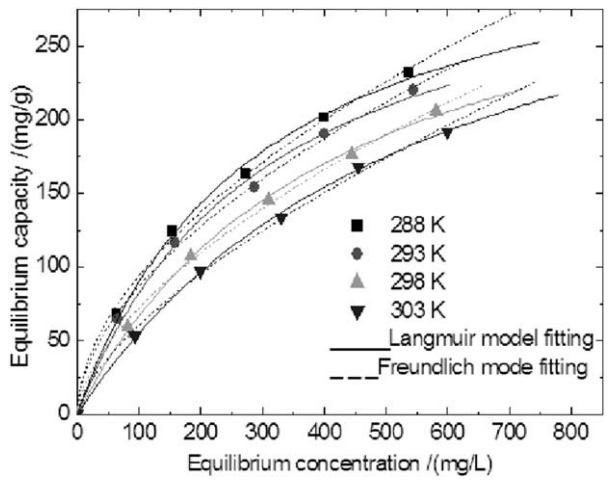

Figure 5. Adsorption isotherms of phenol on HCP–HMTA–AA at 288, 293, 298, and 303 K.

Following the Clausius-Clapeyron equation:[26,27,29]

$$\frac{d\ln C_e}{dT} = \frac{\Delta H}{RT^2} \quad (5)$$

where ΔH (kJ/mol) is the adsorption enthalpy at a given equilibrium adsorption capacity or a fractional loading (θ, where θ equals q_e'/q_m, and q_e' is the given equilibrium adsorption capacity and q_m is the plotted equilibrium adsorption capacity by Langmuir model), T is the temperature (K) and R is the gas constant [8.314 J/(mol·K)].

Equation (6) can be followed by integration of eq. (5):

$$\ln C_e = -\Delta H/(RT) + C' \quad (6)$$

where C' is the integral constant.

As plotting ln C_e versus $1/T$, all of the isosters are straight lines ($R^2 > 0.98$), and ΔH can be calculated from the slopes of the straight lines. As displayed in Figure 6, the ΔH is shown to be negative, implying the exothermic character of the adsorption process, and this phenomenon is coincident with the above observation. Moreover, ΔH decreased with increasing of the fractional loading, suggesting that HCP–HMTA–AA possesses surface energy heterogeneity.[29] In particular, ΔH can be predicted to be −99.56 kJ/mol at zero fractional loading, which is close to that of PVBA (−91.4 kJ/mol at 5 mg/g of equilibrium adsorption capacity) and much greater than that of PMVBA (−77.08 kJ/mol at 20% of fractional loading).

Hydrogen bonding is proven the main driving force for phenol adsorption on PMVBA.[26,27,41] The oxygen atom of carbonyl group of N-methylacetamide of PMVBA acts as the hydrogen bonding acceptor, and forms hydrogen bonding with the hydrogen atom of hydroxyl group of phenol. The hydrogen bonding is frequently in the range of 8–50 kJ/mol.[42] The present adsorption enthalpy for the phenol adsorption on HCP–HMTA–AA is −99.56 kJ/mol at zero fractional loading, much greater than the

Table IV. The Fitted Parameters of the Isotherm Data for Phenol Adsorption on HCP-HMTA-AA by the Langmuir and Freundlich Models

	Langmuir model			Freundlich model		
	K_L (L/g)	q_m (mg/g)	R^2	K_F ([(mg/g) (L/mg)$^{1/n}$])	n	R^2
288 K	3.653	373.1	0.9910	6.546	1.751	0.9970
293 K	3.497	343.6	0.9841	6.111	1.748	0.9980
298 K	2.511	340.1	0.9924	3.932	1.596	0.9974
303 K	1.767	327.8	0.9952	2.368	1.442	0.9976

hydrogen bonding. It is deduced that multiple hydrogen bonding is the main reason. Li et al. proposed that multiple hydrogen bonding is the main driving force for phenol adsorption on PVBA,[28] while they did not give direct evidence. Here, we performed theoretical calculation to demonstrate the above conclusion.

We used N-methylacetamide to simulate HCP–HMTA–AA, and this simulation feasible.[26] Figure 7 indicates that, for the admixture of N-methylacetamide and phenol, double hydrogen bonding is formed between N-methylacetamide and phenol. The first hydrogen bonding is strong, and it is formed between the oxygen atom of carbonyl of acetamide group and the hydrogen atom of hydroxyl group of phenol. This strong hydrogen bonding has its hydrogen bonding bond length (O···H–O) of 1.708Å and bond angle (∠OHO) of 155.4°, respectively. The second hydrogen bonding is rather weak, and this weak hydrogen bonding is related to the hydrogen atom of amino of acetamide group and the oxygen atom of hydroxyl group of phenol, and it has its hydrogen bonding bond length (O···H–N) of 2.076Å and bond angle (∠OHN) of 139.6°, respectively. In particular, the hydrogen bonding energy is calculated to be −68.28 kJ/mol, much greater than the single hydrogen bonding energy between N, N-dimethylacetamide (simulation of PMVBA) and phenol (−55.23 kJ/mol). The theoretical value of hydrogen bonding energy is lower than the experimental one. However, only a single hydrogen bonding is existent between PMVBA and phenol,

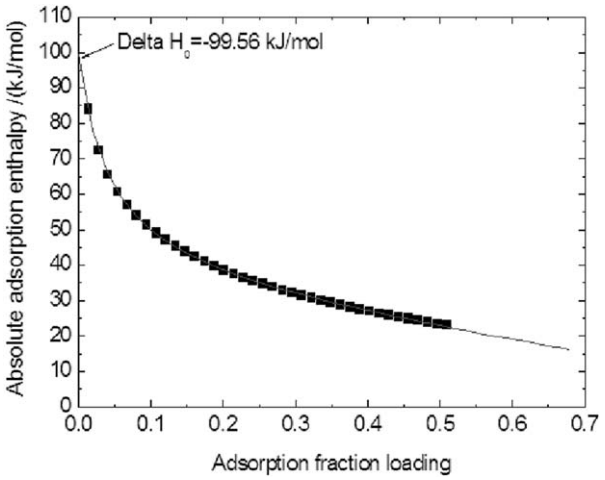

Figure 6. Plotting of the absolute adsorption enthalpy with the fractional loading (θ) for phenol adsorption on HCP–HMTA–AA.

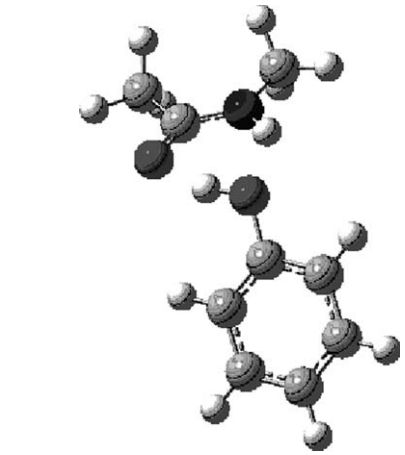

Figure 7. The multiple hydrogen bonding model for N-methylacetamide and phenol.

while a multiple hydrogen bonding exists between HCP–HMTA–AA, PVBA and phenol. Moreover, it is interesting to observe that the hydrogen and oxygen atoms of hydroxyl group of phenol are almost in the same plane of the involved carbon, nitrogen and oxygen atoms of N-methylacetamide, the dihedral angle is determined to be 7°. That is, an approximately planar hexahydric ring is certainly formed between N-methylacetamide and phenol, and two hydrogen bonding are considered in the approximately planar hexahydric ring.

Dynamic Adsorption and Desorption

Figure 8 displays the breakthrough profile for phenol adsorption on HCP–HMTA–AA resin column, the initial concentration of phenol was 946.2 mg/L and the flow rate was 48 mL/h, respectively. As shown in Figure 8, the breakthrough point ($C/C_0 = 0.05$) of phenol on HCP–HMTA–AA resin column was 902.4 mL, and the total dynamic capacity of phenol on HCP–HMTA–AA can be estimated to be 973.2 mg. By considering

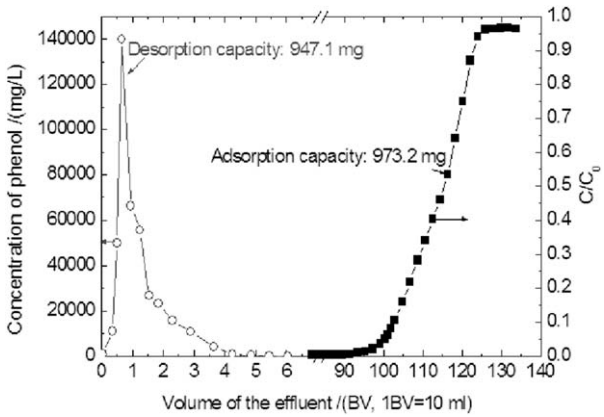

Figure 8. Dynamic adsorption and desorption curves of phenol on HCP–HMTA–AA resin column (Dynamic adsorption: 3.34 g of HCP–HMTA–AA resin was used and the wetted volume of the resin was 10 mL; C_0 was 946.2 mg/L and the flow rate was 48 mL/h; the performed temperature was set as the room temperature. Dynamic desorption: a mixed solution including 50% of ethanol (v/v) and 0.01 mol/L of sodium hydroxide (w/v) was applied as the desorption solvent and the flow rate was 30 mL/h).

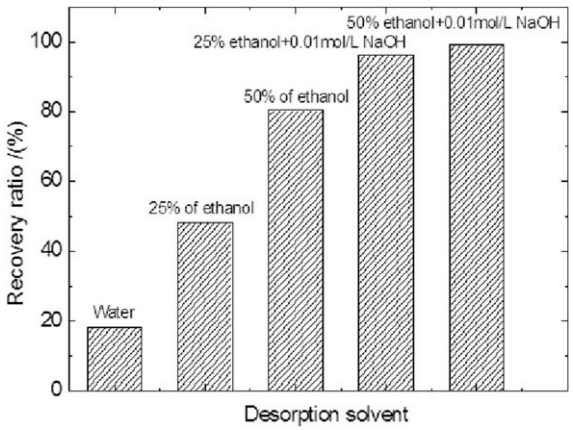

Figure 9. The recovery ratio of different solvents for desorption of phenol from HCP–HMTA–AA resin column.

the mass of the resin column (3.34 g), the dynamic capacity can be determined to be 291.3 mg/g, confirming that HCP–HMTA–AA is an efficient resin for phenol adsorption. In addition, the dynamic capacity is close to the extrapolated value by the Langmuir (268.9 mg/g) and Freundlich model (319.2 mg/g).

After the breakthrough run, different solvents are employed for regeneration of the resin column, and the desorption ratio of the resin column by different solvents is displayed in Figure 9. It is evident that water can partly regenerate the resin column, and 18.13% of phenol is desorbed from the resin column as water is applied as the desorption solvent. Ethanol is shown an effective solvent for regeneration of the resin column, and 48.22% of phenol is recovered by 25% of ethanol (v/v), which may be from the miscible ability of ethanol with phenol. In addition, increasing the concentration of ethanol induces an increased desorption ratio. In particular, addition of sodium hydroxide in ethanol can further improve the desorption ratio, and 99.3% of phenol can be recovered as 50% of ethanol (v/v) and 0.01 mol/L of sodium hydroxide is used as the desorption solvent. Hence, a mixed solution including 50% of ethanol (v/v) and 0.01 mol/L of sodium hydroxide (w/v) is applied as the desorption solvent in the dynamic desorption. At a flow rate of 30 mL/h, only 50 mL of the desorption solvent is enough for regeneration of the resin column, and the dynamic desorption capacity is calculated to be 947.1 mg (Figure 8), very close to the dynamic capacity (973.2 mg). HCP–HMTA–AA is repeatedly used for five cycles of continuous adsorption–desorption process, the equilibrium adsorption capacity for the five time reaches 94.2% of the initial equilibrium adsorption capacity (Figure 10), and the adsorbed phenol can be almost desorbed every time. HCP–HMTA–AA exhibits good reusability with good regeneration behaviors.

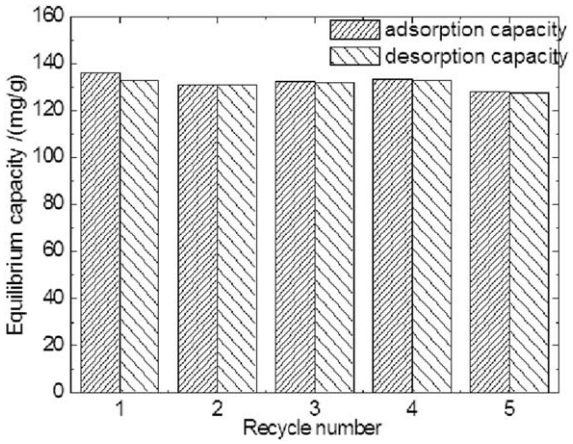

Figure 10. Effect of recycle number on the equilibrium adsorption/desorption capacity of phenol on HCP–HMTA–AA from aqueous solution.

CONCLUSION

A novel acetamide-modified hyper-cross-linked resin, HCP–HMTA–AA, was successfully synthesized in this study, 0.517 mmol/g of —$NHCOCH_3$ and 0.187 mmol/g of —NH_2 groups were modified on the surface of HCP–HMTA–AA. 539.0 m^2/g of t-plot micropore surface area and 0.2982 cm^3/g of t-plot micropore volume were determined for HCP–HMTA–AA, implied that micro/mesopores were predominant for HCP–HMTA–AA. Freundlich model characterized the equilibrium data well better than the Langmuir model, the isosertic adsorption enthalpy could be predicted to be −99.56 kJ/mol at zero fractional loading, and multiple hydrogen bonding and an approximately planar hexahydric ring was formed between HCP–HMTA–AA and phenol. At an initial concentration of 946.2 mg/L and a flow rate of 48 mL/h, the dynamic capacity was measured to be 291.3 mg/g, close to the extrapolated value by the Langmuir (268.9 mg/g) and Freundlich model (319.2 mg/g), and the resin could be almost desorbed by a mixed solvent including 50% of ethanol (v/v) and 0.01 mol/L of sodium hydroxide (w/v).

ACKNOWLEDGMENTS

The financial supports by the National Natural Science Foundation of China (No. 21176063, 21376275, 21174163, and 213111014) are gratefully acknowledged.

REFERENCES

1. Ahmaruzzaman, Md. *Adv. Colloid Interf. Sci.* **2008**, *143*, 48.
2. Caetano, M.; Valderrama, C.; Farran, A.; Cortina, J. L. *J. Colloid Interface Sci.* **2009**, *338*, 402.
3. Srihari, V.; Das, A. *Ecotoxicol. Environ. Saf.* **2008**, *71*, 274.
4. Ipek, I.; Kabay, N.; Yüksel, M.; Yapc, D.; Yüksel, Ü. *Desalination* **2012**, *306*, 24.
5. Ahmaruzzaman, Md.; Gayatri, S. L. *J. Chem. Eng. Data* **2011**, *56*, 3004.
6. Ayranci, E.; Duman, O. *J. Hazard. Mater.* **2005**, *124*, 125.
7. Chern, J. M.; Chein, Y. W. *Water Res.* **2002**, *36*, 647.
8. Rogozhin, S. V.; Davankov, V. A.; Tsyurupa, M. P. USSR Pat. 299165, **1969**.
9. Tsyurupa, M. P.; Davankov, V. A. *React. Funct. Polym.* **2002**, *53*, 193.

10. Li, A. M.; Zhang, Q. X.; Zhang, G. C.; Chen, J. L.; Fei, Z. H.; Liu, F. Q. *Chemosphere* **2002**, *47*, 981.
11. He, C. L.; Huang, J. H.; Yan, C.; Liu, J. B.; Deng, L. B.; Huang, K. L. *J. Hazard. Mater.* **2010**, *180*, 634.
12. Maya, F.; Svec, F. *Polymer* **2014**, *55*, 340.
13. Wood, C. D.; Tan, B.; Trewin, A.; Niu, H.; Bradshaw, D.; Rosseinsky, M. J.; Khimyak, Y. Z.; Campbell, N. L.; Kirk, R.; Stöckel, E.; Cooper, A. I. *Chem. Mater.* **2007**, *19*, 2034.
14. Li, B.; Huang, X.; Liang, L.; Tan, B. *J. Mater. Chem.* **2010**, *20*, 7444.
15. Tsyurupa, M. P.; Davankov, V. A. *React. Funct. Polym.* **2006**, *66*, 768.
16. Long, C.; Liu, P.; Li, Y.; Li, A. M.; Zhang, Q. X. *Environ. Sci. Technol.* **2011**, *45*, 4506.
17. Wang, X. M.; Dai, K. L.; Chen, L. M.; Huang, J. H.; Liu, Y. N. *Chem. Eng. J.* **2014**, *242*, 19.
18. Oh, C. G.; Ahn, J. H.; Ihm, S. K. *React. Funct. Polym.* **2003**, *57*, 103.
19. Ahn, J. H.; Jang, J. E.; Oh, C. G.; Ihm, S. K.; Cortez, J.; Sherrington, D. C. *Macromolecules* **2006**, *39*, 627.
20. Davankov, V. A.; Tsyurupa, M. P. *React. Polym.* **1990**, *13*, 27.
21. Macintyre, F. S.; Sherrington, D. C.; Tetley, L. *Macromolecules* **2006**, *39*, 5381.
22. Tsyurupa, M. P.; Davankov, V. A. *React. Funct. Polym.* **2002**, *53*, 193.
23. Li, C. Y.; Xu, M. W.; Sun, X. C.; Han, S.; Wu, X. F.; Liu, Y. N.; Huang, J. H.; Deng, S. G. *Chem. Eng. J.* **2013**, *229*, 20.
24. Zhang, M. C.; Li, A. M.; Zhou, Q.; Shuang, C. D.; Zhou, W. W.; Wang, M. Q. *Micropor. Mesopor. Mater.* **2014**, *184*, 105.
25. Fan, J.; Yang, W.; Li, A. *React. Funct. Polym.* **2011**, *71*, 994.
26. Xu, M. C.; Zhou, Y.; Huang, J. H. *J. Colloid Interf. Sci.* **2008**, *327*, 9.
27. Huang, J. H.; Zhou, Y.; Huang, K. L.; Liu, S. Q.; Luo, Q.; Xu, M. C. *J. Colloid Interf. Sci.* **2007**, *316*, 10.
28. Huang, J. H.; Jin, X. J.; Deng, S. G. *Chem. Eng. J.* **2012**, *192*, 192.
29. Li, H. T.; Xu, M. C.; Shi, Z. Q.; He, B. L. *J. Colloid Interf. Sci.* **2004**, *271*, 47.
30. He, B. L.; Huang, W. Q. Ion Exchange and Adsorption Resin; Shanghai Science and Technology Education Press: Shanghai, **1995**.
31. Wu, C. P.; Zhou, C. H.; Li, F. X. Experiments of Polymeric Chemistry; Anhui Science and Technology Press: Hefei, **1987**.
32. Huang, J. H.; Jin, X. Y.; Mao, J. L.; Yuan, B.; Deng, R. J.; Deng, S. G. *J. Hazard. Mater.* **2012**, *217*, 406.
33. Devaky, K. S.; Pilla, V. N. R. *Eur. Polym. J.* **1988**, *24*, 209.
34. Meng, G. H.; Li, A. M.; Yang, W. B.; Liu, F. Q.; Yang, X.; Zhang, Q. X. *Eur. Polym. J.* **2007**, *43*, 2732.
35. Wang, J. T.; Hu, Q. M.; Zhang, B. S.; Wang, Y. M. Organic Chemistry; Nankai University Press: Tianjing, **1998**.
36. Huang, J. H. *J. Appl. Polym. Sci.* **2011**, *121*, 3717.
37. Gokce, Y.; Aktas, Z. *Appl. Surf. Sci.* **2014**, *313*, 352.
38. Yang, G.; Chen, H. L.; Qin, H. D.; Feng, Y. J. *Appl. Surf. Sci.* **2014**, *293*, 299.
39. Langmuir, I. *J. Am. Chem. Soc.* **1916**, *38*, 2221.
40. H. M. F. Z. *Phys. Chem.* **1906**, *57A*, 385.
41. Huang, J. H.; Huang, K. L.; Liu, S. Q.; Luo, Q.; Xu, M. C. *J. Colloid Interf. Sci.* **2007**, *315*, 407.
42. Wang, Q. W.; Yang, Y. H.; Gao, H. B. Problems of hydrogen bonding in organic chemistry, Tianjin University Press: Tianjin, **1993**.